Time Scale for Rapid Draining of a Surficial Lake into the Greenland Ice Sheet

James R. Rice *
Professor, Fellow of ASME, School of Engineering and Applied Sciences,
and Department of Earth and Planetary Sciences,
Harvard University, Cambridge, MA 02138, Email: rice@seas.harvard.edu

Victor C. Tsai
Assistant Professor, Seismological Laboratory
California Institute of Technology, Pasadena, CA 91125, Email: tsai@caltech.edu

Matheus C. Fernandes
Graduate Research Assistant, Student Member of ASME
School of Engineering and Applied Sciences
Harvard University, Cambridge, MA 02138, Email: fernandes@seas.harvard.edu

John D. Platt
Postdoctoral Fellow, Department of Terrestrial Magnetism
Carnegie Institution of Science, Washington, DC 20015, Email: jplatt@dtm.ciw.edu

ASME Journal of Applied Mechanics, paper JAM-15-1063 for special issue honoring Alan Needleman, originally submitted 31 Jan 2015, tentatively accepted 23 Feb 2015, submitted with final revisions 11 Mar 2015, final approval for publication 2 Apr 2015. doi:10.1115/1.4030325

A 2008 report by Das et al. documented the rapid drainage during summer 2006 of a supra-glacial lake, of approximately 44×10^6 cubic meters, into the Greenland Ice Sheet over a time scale moderately longer than 1 hour. The lake had been instrumented to record the time-dependent fall of water level, and the uplift of the ice nearby. Liquid water, denser than ice, was presumed to have descended through the sheet along a crevasse system, and spread along the bed as a hydraulic facture. That event led two of the present authors to initiate modeling studies on such natural hydraulic fractures. Building on results of those studies, we attempt to better explain the time evolution of such a drainage event. We find that the estimated time has a strong dependence on how much a pre-existing crack/crevasse system, acting as a feeder channel to the bed, has opened by slow creep prior to the time at which a basal hydraulic fracture nucleates. We quantify the process and identify appropriate parameter ranges, particularly of the average temperature of the ice beneath the lake (important for the slow creep opening of the crevasse). We show that average ice temperatures 5 to 7°C below melting allow such rapid drainage on a time scale which agrees well with the 2006 observations.

*Corresponding author

1 Introduction

As annual late spring and summer temperatures affect the Greenland ice sheet, there is extensive meltwater generation and flow over its surface. Observations show that this water often collects in surficial lakes. A particular lake, located near the western margin of Greenland (68.72°N, 49.50°W), was instrumented during 2006 by Das et al. [1]; see Fig. 1 and Fig. 2 based on their work. It provided a remarkably clear record of the rapid disappearance of the lake's water into the ice. Our previous studies [2, 3, 4] supported quantitatively their [1] suggestion that the liquid had proceeded downward along a major crevasse system extending below the lake, through a process suggested by Weertman [5], and then propagated as a turbulently driven hydraulic fracture along the ice/rock interface at the base (see below).

The basic facts about the supraglacial meltwater lake are as follows [1] (Fig. 1 and Fig. 2):

1. The lake began filling in July 2006.
2. The lake surface level reached a maximum at $\sim$ 0:00 hr on 29 July 2006.
3. At that maximum, the lake volume was $\sim$ 44 x 10^6 m^3, and surface area $\sim$5.6 km^2.
4. Shortly after $\sim$ 0:00 the level (marked by the "Falling lake level" curve in Fig. 2, and read on the right-

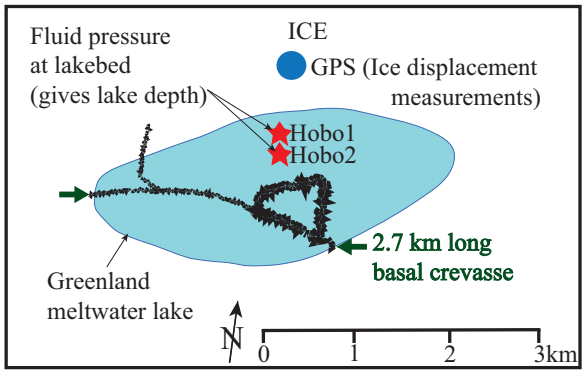

Fig. 1. Sketch illustrating early October 2006 Synthetic Aperture Radar (SAR) image overlaid with the NASA Moderate Resolution Imaging Spectroradiometer (MODIS) image, showing the lake extent (blue) on 29 July 2006. This figure was redrawn here to approximately duplicate the features in Das et al. [1]. A GPS station measuring the ice displacement was located $\sim 1/4$ km from the lake shore. Hobo instruments located on the lakebed measured fluid pressure, from which lake depth versus time was inferred.

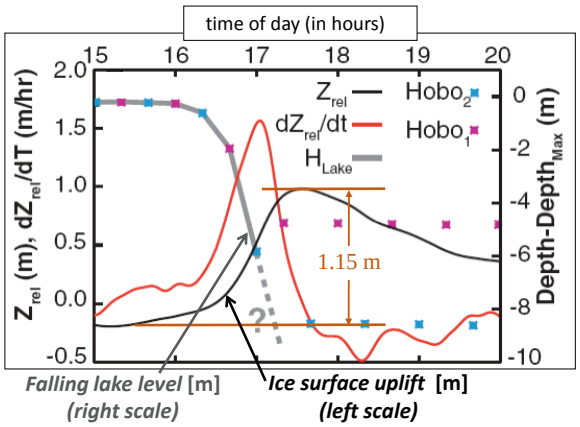

Fig. 2. Data from the 2006 lake drainage event reproduced from Das et al. [1] with additional labeling by the authors: Lake level vs. time shown, as inferred from water-pressure loggers (Fig. 1) Hobo1 and Hobo2 (blue and magenta symbols and gray line, referred to right vertical axis; the dashed gray line is a linear fit to the last two lake-level measurements before loggers were left dry, suggesting that the lake drained completely prior to 17:30 UTC.). Uplift at GPS site (Fig. 1), acquired with 5-min temporal resolution (black line, referred to left vertical axis; red line shows rate of uplift).

side scale) was observed to slowly/steadily fall at ∼15 mm/hr.

5. The rate of fall became much more rapid shortly after 16:00 hr.
6. Then, within $\sim$ 1.5 hr, the lakewater rapidly disappeared into the ice, with the lake surface falling at a maximum rate of $\sim$ 12 m/hr, with the maximum volumetric discharge rate Q $>$ 10,000 m^3/s, and average rate Q $\sim$ 8,700 m^3/s during the discharge. (In comparison, for the Niagara River leading to Niagara Falls, the average Q is $\sim$ 5,750 m^3/s [6]).

The lake level H_{Lake} during drainage was determined from two pressure meters (Hobo 1 and 2), see Fig. 1, although these were left dry (Fig. 2, curve denoted H_{Lake}, with axis scale on right side) well before full drainage. A GPS instrument was placed ∼0.7 km from the lake edge, but yet further from the ∼2.7 km long crevasse system (Fig. 1) through which the water is presumed to have drained. The uplift it recorded is labeled Z_{rel}, the black curve with axis scale on the left, and its time rate is shown in red. We have marked the 1.15 m maximum transient uplift Z_{rel}, attained at $\sim$ 17:40 hr, whereas the uplift rate dZ_{rel}/dt is maximum at $\sim$ 17:00 hr.

A simple calculation suggests that the water entering beneath the ice sheet, transiently lifting it from its bed, does so by a strongly turbulent flow. Let R be the radius of the subglacial fracture, approximated for simplicity as circular, near the condition of full lake discharge. Then $\pi R^2 \times$ uplift of 1.15m $\approx$ the lake volume of 44 x 10^6 m^3, giving $R \approx 3.5$ km at full drainage. Since that takes about 1.2 hr to occur, the average fracture growth speed along the interface can be approximated as R/1.2 hr $\approx$ 3 km/hr. Recalling that the kinematic viscosity of water is $\sim 10^{-6}$m^2/s , the Reynolds number for flow in the fracture is

$$Re = (3\text{km/hr} \times 1.15\text{m})/(10^{-6}\text{m}^2/\text{s}) \approx 8 \times 10^5 \qquad (1)$$

and numbers in excess of 10^5 would still be appropriate if we reduced the assumed gap size significantly, as may be appropriate for the earlier phases of the fracture propagation.

However, although our initial attempt [2] to explain the remarkably short time scale for the lake disappearance yielded order-of-magnitude agreement, it did not agree precisely with observations. Ice, like all solids, responds elastically on short time scales, although creep deformation becomes dominant on longer time scales [7]. The assumption of elastic response seems appropriate over the short time scale of the lake drainage, of order 1.5 hrs in Fig. 1. Nevertheless, we argue here that a critical aspect of the drainage process was developing by creep flow, well before the onset of rapid drainage. That creep, a process to which Needleman and co-workers [8, 9] have contributed insightful computational methodology in other contexts, plays an important role in determining the estimated time scale of the lake drainage.

2 Analysis

To model the drainage event, or at least a simple but tractable representation of it, we adopt the solution of [3] for an ice sheet of uniform thickness H ($\approx$ 1 km), see Fig. 3, in which a vertical crevasse connected to the lake supplies water to a growing opening gap (basal fracture) along the bed, with fluid inlet pressure $p_{inlet}(t)$ at the entry point. The equation system solved in [3] generalized that in [2] to allow the crack

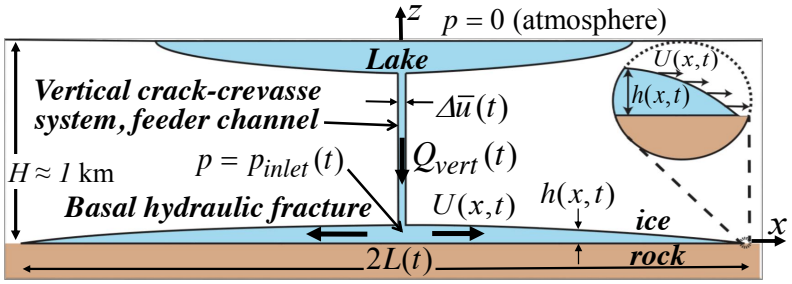

Fig. 3. Schematic of subglacial drainage system showing the vertical influx $Q_{vert}(t)$ from the lake through the crack-crevasse system feeder channel, and the resulting water injection along the ice-bed interface. The feeder channel horizontal opening $\Delta\bar{u}$ includes contributions from elastic opening, $\Delta\bar{u}^{el}$, linearly proportional to the current fluid pressure, and prior creep opening, $\Delta\bar{u}^{cr}$, which accumulated over an extended time before the rapid drainage. The ice sheet height H is much larger than the lake depth and the basal fracture opening $h(x,t)$. Additionally, the lake diameter is also significantly smaller than the ultimate horizontal spread of $2L(t)$ of the basal hydraulic fracture.

half-length $L(t)$ to be comparable to and several times larger than ice thickness H (whereas [2] presented a self-similar solution for the range $L(t)/H << 1$, i.e., effectively for a fracture at the base of an unbounded domain).

The modeling of [3] assumes, as justified in retrospect, that for purposes of calculating the elastic deformation and hence the crack opening displacement, that only the local fluid pressure $p(x,t)$ $[= -\sigma_{zz}(x,z=0,t)]$ need be considered. That is because it is normally far greater than the shear tractions $\tau_{wall}(x,t)$ $[= -\sigma_{zx}(x,z=0,t)]$ exerted along the walls of the fracture from resistance to fluid infiltration. To solve for the crack opening in a manner which solves the elasticity equations in 2D plane strain, and meets the traction-free surface boundary conditions at $z=H$, the numerical integral equation formulation of Erdogan et al. [10] (with correction of a mis-printed kernel as noted in [11]) was used. That relates the pressure distribution $p(x,t)$ to the crack opening gap $h(x,t)$ at each time t (with inertia neglected because of the slowness of fracture propagation speeds relative to elastic wave speeds). Also, in view of the low fracture toughness of ice, $K_{Ic} \approx 0.1$ MPa, it was judged that toughness became unimportant, in the sense quantified by Garagash and Detournay [12], once crack half-length $L(t)$ was greater than ≈ 10 m. Effectively, over the long length scale of fracture growth ($L > 1$ km), the problem of fracture becomes asymptotically indistinguishable from the problem of lift-off along a non-adhering (zero K_{Ic}) interface.

Elasticity theory under plane strain conditions in the x-z plane, and within the usual approximations of linear elastic theory, relates displacement discontinuities $\Delta u_x(x,t)$ and $\Delta u_z(x,t)$ (along the fracture plane $z=0$, between $x=-L(t)$ and $x=+L(t)$), to the traction stress components acting on that plane and in adjacent material by

$$\left\{ \begin{matrix} \sigma_{zx}(x,z,t)/E' \\ \sigma_{zz}(x,z,t)/E' \end{matrix} \right\} = \int_{-L(t)}^{+L(t)} \begin{pmatrix} K_{xx}(x-x',z) & K_{xz}(x-x',z) \\ K_{zx}(x-x',z) & K_{zz}(x-x',z) \end{pmatrix} \frac{\partial}{\partial x'} \left\{ \begin{matrix} \Delta u_x(x',t) \\ \Delta u_z(x',t) \end{matrix} \right\} dx'. \tag{2}$$

The notation here is that, with $u_\alpha = u_\alpha(x,z,t)$, for $\alpha = x$ or z, $\Delta u_\alpha(x,t) = u_\alpha(x,z=0^+,t) - u_\alpha(x,z=0^-,t)$. The kernels K_{xx}, K_{xz}, K_{zx}, and K_{zz} all vanish on the plane $z=H$, the surface of the ice sheet, so as to meet the traction-free boundary condition. Also, on the plane $z=0$, the diagonal kernels K_{xx} and K_{zz} include terms which are Cauchy singular, like $1/(x-x')$. Here $E' = E/(1-\nu^2)$ where E is Young's modulus and ν is the Poisson ratio. The full form of the kernels as $z \to 0^+$, the upper side of the fracture plane (i.e., the base of the ice sheet), is given by Erdogan et al. [10], although a misprint as identified in [11] must be corrected.

As $z \to 0^+$, $\sigma_{zz}(x,z,t) \to -p$, where p is the local fluid pressure in the fracture, whereas $\sigma_{zx}(x,0,t) \to -\tau_{wall}$, the shear stress resisting the turbulent fluid flow in the fracture. Typically, in such hydraulic fracture situations, $\tau_{wall} << p$ and we follow [3] in neglecting τ_{wall} in comparison to p. Thus, recognizing $\Delta u_z(x,t)$ as $h(x,t)$, the opening gap along the fracture, the hydraulic fracture problem is formulated, like in [3], as

$$\left\{ \begin{matrix} 0 \\ -p(x,t)/E' \end{matrix} \right\} = \int_{-L(t)}^{+L(t)} \begin{pmatrix} K_{xx}(x-x',0^+) & K_{xz}(x-x',0^+) \\ K_{zx}(x-x',0^+) & K_{zz}(x-x',0^+) \end{pmatrix} \frac{\partial}{\partial x'} \left\{ \begin{matrix} \Delta u_x(x',t) \\ h(x',t) \end{matrix} \right\} dx' \tag{3}$$

which ultimately relates the pressure distribution $p(x,t)$ within the fracture to its opening gap $h(x,t)$ along it.

Consistent with the high Reynolds number estimated in Eq. 1, the flow in the fracture is expected to be a turbulent flow in a rough-walled gap. The relevant considerations are, first, that the Darcy-Weisbach friction factor f, for such flows at mean velocity U in rough-walled pipes or channels, is defined by writing the wall shear stress resisting the flow as $\tau_{wall}/(\rho U^2/2) = f/4$ (ρ is the density of the fluid, water in our case). That f may be estimated for the present case of flow in a thin slit by using well-calibrated data for flow in rough-walled cylindrical pipes, reinterpreted for a

slit using the hydraulic radius concept. Following [2], that gives $f \approx 0.143(k/h)^{1/3}$ where k is the amplitude of the wall roughness as an equivalent Nikuradse grain size. An insightful recent discussion on such turbulent flow in rough-walled tubes is given by Gioia and Chakraborty [13]; see also [14].

Observing that the gap h times the pressure gradient $-\partial p/\partial x$ is equilibrated by $2\tau_{wall}$, we have

$$-h\frac{\partial p}{\partial x} = 0.0357\rho U^2 (k/h)^{1/3} \tag{4}$$

(here, ρ is the mass density of the water; we use ρ_{ice} below for the lesser mass density of the ice).

To the preceding Eq. 3 and Eq. 4 we add the conservation of mass,

$$\frac{\partial (hU)}{\partial x} + \frac{\partial h}{\partial t} = 0 \tag{5}$$

to close the system, as the set of equations in fluid pressure p, fracture opening gap h, and fluid velocity U that was formulated and solved numerically in [3] (and earlier for the $L << H$ range in [2]).

3 Application to basal fracture propagation

Here we present the solutions to the above system of equations, as devised in [3], and use them subsequently to address the time scale of glacial under-flooding in the lake drainage event considered.

The rate of fracture propagation along the bed is

$$\frac{dL}{dt} \equiv U_{tip} = \left(\frac{p_{inlet} - \sigma_o}{\rho}\right)^{\frac{1}{2}} \left(\frac{p_{inlet} - \sigma_o}{E'}\right)^{\frac{2}{3}} \left(\frac{L}{k}\right)^{\frac{1}{6}} \phi\left(\frac{L}{H}\right). \tag{6}$$

Here the notation is a reminder that the fracture growth rate is assumed equal to the fluid velocity at the tip, and the function $\phi(L/H)$, as fitted to the numerical results of [3], is

$$\phi(L/H) \approx 5.13[1 + 0.125(L/H) + 0.183(L/H)^2]. \tag{7}$$

The polynomial in L/H in the brackets closely fits results of [3] out to $L/H = 5$, that is to $L \approx 5$km. Here σ_o is given by

$$\sigma_o \equiv \rho_{ice} g H, \tag{8}$$

the overburden pressure of the ice (which p_{inlet} must evidently exceed in order for water to be driven beneath the ice sheet to open the fracture). Note that in the absence of vertical flow, $p_{inlet} = \rho g H$, and since the liquid water density $\rho \approx 1.1\rho_{ice}$, $p_{inlet} > \sigma_o$ under those hydrostatic conditions, which is what drives the water to the bed.

Further, for a given inlet pressure p_{inlet}, the average h_{avg} of the opening gap $h(x,t)$ along $-L(t) < x < +L(t)$, i.e., along the fracture, is expressible in terms of p_{inlet} and L, as

$$h_{avg} \approx 1.72 \frac{p_{inlet} - \sigma_o}{E'} L[1 + 0.517(L/H)^2]. \tag{9}$$

Here the expression in the brackets closely fits numerical results of [3] up to $L/H = 3.5$, but falls about 15 percent too low at $L/H = 5$.

To estimate the volumetric inflow rate Q_{basal} (units [L^3]/[T]) to the bed, we choose some representative width W perpendicular to the diagram of Fig. 3 (i.e., in the unmarked y direction) over which the inflow rate (units [L^2]/[T]) per unit distance perpendicular to the plane of the diagram, calculated from the 2D plane strain solution of [3], may be assumed to apply approximately. We take $W = 3$km for that width, noting that the major crevasse marked in Fig. 1 extends over a length of 2.7 km along the lake bed, and anticipating that the flow extended the lift of the ice off from its bed somewhat beyond the end of that feature. (Ultimately, a 3D analysis is needed, but that is well beyond the scope of this paper.) Thus, noting that $2LWh_{avg}$ is the volume of water in the subglacial fracture,

$$\begin{aligned} Q_{basal} &= \frac{d(2LWh_{avg})}{dt} \\ &= 6.88 \frac{(p_{inlet} - \sigma_o)}{E'} WL \left(1 + 1.034 \frac{L^2}{H^2}\right) \frac{dL}{dt} \end{aligned} \tag{10}$$

where dL/dt is given by Eq. 6, with Eq. 7, above. We note that for a given L/H, $dL/dt \propto (p_{inlet} - \sigma_o)^{7/6}$, and thus

$$Q_{basal} \propto (p_{inlet} - \sigma_o)^{13/6}. \tag{11}$$

4 Coupling to lake water supply to the bed by a vertical crack-crevasses system

By mass conservation, the volumetric flow rate Q_{basal} into the basal fracture must equal Q_{vert} (see Fig. 3), the volumetric flow rate at which lake water flows down the vertical crack-crevasse system (which forms a feeder channel to the basal fracture). We assume that this vertical system has a width in the y direction (perpendicular to the plane of the diagram in Fig.3) which is the same width W as adopted above for the basal fracture. Also, for simplicity in making elementary estimates of the lake drainage time scale, we model this vertical feeder channel as having a spatially uniform opening gap $\Delta\bar{u} = \Delta\bar{u}(t)$, thought of as the area-averaged opening of a vertical crack of depth $H \approx 1$ km in the z direction and width $W \approx 3$ km in the y direction, with faces loaded by the area-average pressures.

We determine the vertical flux using an elementary balance of forces on a vertical slab of water from the lake, of area HW and thickness $\Delta\bar{u}$, moving downward with velocity

U_{vert} ($= Q_{vert}/W\Delta\bar{u}$). The flow is driven downward by the slab weight $\rho g H W \Delta\bar{u}$, which is balanced by the sum of the upward force $p_{inlet} W \Delta\bar{u}$ at the base of the slab and the shear forces from the wall shear stresses on the two vertical boundaries summing to $2\tau_{wall} HW$ where $\tau_{wall} = \rho(f/8)U_{vert}^2$ and $f = 0.143(k/\Delta\bar{u})^{1/3}$. Balancing these forces leads to,

$$\rho g H W \Delta\bar{u} = (f/4)\rho U_{vert}^2 HW + p_{inlet} W \Delta\bar{u}, \qquad (12)$$

which can be rearranged to give the formula for the vertical flux

$$Q_{vert} \approx 5.29 \left(1 - \frac{p_{inlet}}{\rho g H}\right)^{1/2} W \Delta\bar{u}^{3/2} g^{1/2} \left(\frac{\Delta\bar{u}}{k}\right)^{1/6}. \qquad (13)$$

In a somewhat similar attempt to link flow down the vertical crevasse to flow into the basal fracture, Tsai and Rice [2] assumed, in view of the relatively short time scale (< 1.5 hr) of rapid drainage, purely elastic response of the vertical crevasse, with its opening being proportional to the difference between the average pressure $p_{inlet}/2$ in the crevasse and the corresponding average $\sigma_o/2$ for the far-field horizontal stress in the ice. That led to the unphysical result of eventual complete crevasse closure when assuming purely elastic response of the ice (which is discussed below).

To more accurately model the drainage, particularly regarding the previous assumption of purely elastic ice deformation, we allow here for the possibility of significant creep opening of the crevasse. To motivate this, recall that slow falling of the lake level was observed for ≈ 16 hrs before the rapid break-out. We interpret that fact here as evidence that the crevasse system may have been highly pressurized before nucleation of the propagating basal fracture at the bed. Thus, we quantify this creep opening of the crevasse before nucleation of the basal fracture. (That nucleation process would, of course, be sensitive to the value of K_{Ic}, or some generalization of it for the ice-rock interface, but we are not able to address it here.) Specifically, we write the crevasse opening $\Delta\bar{u}$ as having an elastic part plus a creep part,

$$\Delta\bar{u} = \Delta\bar{u}^{el} + \Delta\bar{u}^{cr}. \qquad (14)$$

The creep part $\Delta\bar{u}^{cr}$ will depend on how long the crevasse faces have been pressurized prior to basal fracture nucleation, and is assumed to not change significantly during the short time scale of the lake drainage.

The elastic average opening can be derived from a 2D plane strain elastic solution for a crack of length W, opened by uniform pressure taken as $p_{inlet}/2$, in a medium under far-field compressive stress $\sigma_o/2$

$$\Delta\bar{u}^{el} = \frac{\pi(p_{inlet} - \sigma_o)}{4E'} W. \qquad (15)$$

We define C as the ratio of the prior creep opening $\Delta\bar{u}^{cr}$ over the 16 hours of slow drainage to the elastic opening $\Delta\bar{u}^{el}$. In that comparison both are evaluated for hydrostatic pressure $p_{inlet} = \rho g H$ (see Eq. 17 to follow). Inserting this formula for the average conduit opening into our formula for the vertical flux given in Eq. 13, we can write Q_{vert} as a function of p_{inlet} alone. This is shown in Fig. 4 for the parameters given in Tab. 1. We see that the vertical flux increases with C and has a non-monotonic dependence on the inlet pressure. Furthermore, Q_{vert} vanishes when the inlet pressure is equal to $\rho g H$. This figure nicely highlights the competing physical processes that control the flux through the vertical conduit. On the one hand, raising the inlet pressure increases elastic opening of the conduit promoting additional flow. However, raising the inlet pressure also lowers the pressure gradient driving flow, thus suppressing flow. Balancing these two considerations leads to peak fluxes that occur for an intermediate inlet pressure lying between σ_o ($= \rho_{ice} g H$) and $\rho g H$. Note that for $C = 0$ – corresponding to a conduit that undergoes only elastic opening – we also see low fluxes for inlet pressures near $\sigma_o = \rho_{ice} g H$ because the conduit closure chokes the flow.

To estimate the prior creep opening, we represent the creep deformation of the ice sheet by the Glen law form typically adopted in glaciology [7]. This is $d\gamma/dt = 2A_{cr}(T)\tau^n$, with $n = 3$, where τ is the Mises equivalent shear stress, based on the second invariant of the deviatoric stress tensor $s_{\alpha\beta}$, and $d\gamma/dt$ is the equivalent engineering shear strain rate, with the trace of the creep strain rate vanishing (no volumetric creep strain) and with components of deviatoric strain rate being in proportion to one another just as are components of $s_{\alpha\beta}$. Recommended values of $A_{cr}(T)$ are given by Cuffey and Paterson [7], and within the simplicity of our modeling, we evaluate $A_{cr}(T)$ based on a single value of T, hoped to be representative of ice temperatures in the vicinity of the lake and crevasse system. We note that $A_{cr}(T)$ remains finite for the solid phase of ice at its melting temperature.

Although there is no general analytical solution for crack opening in a material undergoing power law creep (except in the linear viscous case), we use the following approach. Based on solutions for pressurized circular holes, elliptical holes, and flat cracks in the $n = 1$ linear viscous case (analogous to familiar linear elastic solutions, but evaluated with $\nu = 1/2$), and the Nye [15] solution for a pressurized circular hole in a power law creeping material, Fernandes and Rice (in progress) have conjectured that the average creep opening rate of a pressurized crack of length W in plane strain, opened by uniform pressure taken as $p_{inlet}/2$, in a power-law creeping solid under far-field compressive stress $\sigma_o/2$, could be represented as

$$\frac{d\Delta\bar{u}^{cr}}{dt} = \kappa(n)\frac{\pi}{2} A_{cr}(T) \left(\frac{p_{inlet} - \sigma_o}{2n}\right)^n W \qquad (16)$$

where $\kappa(n)$ is a correction factor depending on n, which is expected to be close to 1.0 (and is 1.0 in the $n = 1$ case).

In numerical simulations we compared results from the

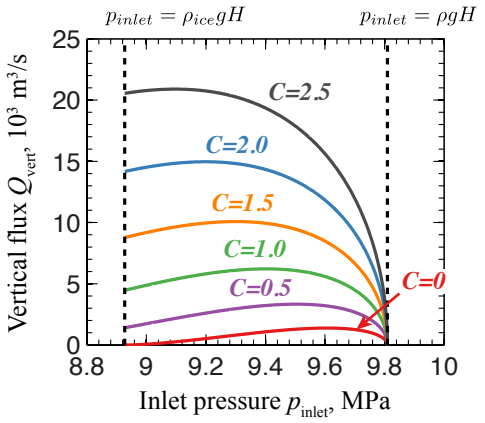

Fig. 4. Dependence of flow rate on inlet pressure for several values of the creep parameter C. In the model, the flow begins at $p_{inlet} = \rho gH$ (hydrostatic pressure), but then the pressure drops as flow rate develops, until the pressure p_{inlet} falls to the ice overburden pressure $\rho_{ice} gH$.

above approximation to a plane-strain finite element model of a pressurized crack using *ABAQUS*. That was formulated as a Maxwell model (elastic and viscous elements in series, where the viscous elements satisfy power law creep), so that when solved within small geometry change assumptions, the displacement rates converge in time to those of a purely viscous material. This approach allows the model to respond to suddenly applied and sustained boundary loading but on a time scale before the crack has opened enough to respond differently from a straight cut. In order to isolate the creep strain rate using the *ABAQUS* elastic plus creep deformation formulation, we waited long enough for essentially steady state creep strain rate to be achieved and elastic relaxation to be completed. See [8,9] for other computational approaches to creep flow. The simulation was benchmarked using two simple tests: (1) Comparing the opening rate of the crack under linear viscous deformation ($n = 1$) to the known analytical solution. Results yield an average nominal nodal error of 0.03 % with a maximum nodal error of 0.1% nearest the crack tip. (2) Using a model assuming a nonlinear rheology ($n = 3$) generate results which were found to compare favorably to the HRR field described by Hutchinson [16] and Rice and Rosengren [17]. By comparing the approximation in Eq. 16 to the numerical solution attained from the *ABAQUS* model, the correction factor $\kappa(n)$ was found, for the $n = 3$ case of interest in this study, to be $\kappa(3) \approx 0.8$.

We estimate $\Delta\bar{u}^{cr}$ at the time of basal fracture nucleation, after approximately 16 hours of slow leakage from the lake, by assuming hydrostatic pressurization of the vertical crevasse system ($p_{inlet} = \rho gH$) for that 16 hour period, hence multiplying $d\Delta\bar{u}^{cr}/dt$ above by 16 hours. As noted, a scale for the resulting $\Delta\bar{u}^{cr}$ is to compare it to the $\Delta\bar{u}^{el}$ corresponding to hydrostatic pressurization of the vertical crevasse, giving C as

$$C = \left(\Delta\bar{u}^{cr}|^{t=16\text{hr}}_{p_{inlet}=\rho gH}\right) \Big/ \left(\Delta\bar{u}^{el}|_{p_{inlet}=\rho gH}\right). \qquad (17)$$

Note that C scales linearly with time t of hydrostatic pressure, with $A_{cr}(T)$, and with H^2 (when $n = 3$). Also, $A_{cr}(T)$ has a weak dependence on ice pressure P [7] which we choose as $P = \sigma_o/2$. Assuming H = 1 km, $E' \approx 6.8$ GPa, $n = 3$, and $\kappa(3) = 0.8$, we consider (being mindful that, as we show in the next section, the best-fitting C to match the discharge data are in the range of $C = 1.5$ to 2.0) average ice temperatures in the range -7.0^oC to -5.0^oC. The corresponding A_{cr} are $A_{cr}(-7^o\text{C}) = 6.32 \times 10^{-25}\text{s}^{-1}\text{Pa}^{-3}$ and $A_{cr}(-5^o\text{C}) = 9.31 \times 10^{-25}\text{s}^{-1}\text{Pa}^{-3}$ With those parameters, and with $H = 1$ km, and standard values of ρ and ρ_{ice}, we obtain $C = 1.42$ at -7.0^oC , and $C = 2.11$ at -5.0^oC, which closely bracket that preferred range of C. Similarly, we obtain temperatures corresponding to relevant C values of $C = 1.50$ as $T = -6.75^\circ$C and $C = 2.00$ as $T = -5.27^\circ$C (see Tab. 1).

In the calculations of the next section, we recognize that the creep opening does not change appreciably during the short time scale of lake drainage, and therefore represent the total crevasse opening $\Delta\bar{u}$ (as needed in Eq. 12 above to characterize resistance to flow down the crevasse) as

$$\Delta\bar{u} = \frac{\pi(p_{inlet} - \sigma_o)}{4E'} W + C\frac{\pi(\rho gH - \sigma_o)}{4E'} W \qquad (18)$$

where $\sigma_o = \rho_{ice} gH$. A recent study addresses in another context how a pre-existing subglacial drainage system interacts with fluid penetration along it [18].

5 Estimating the time scale for lake drainage

In this section we estimate the time scale for lake drainage using our model for combined flow in the vertical conduit and basal fracture. Eq. 6 is solved for the evolution of the basal fracture using an inlet pressure p_{inlet} found by coupling the vertical conduit with the basal fracture through

$$Q_{basal} = Q_{vert}. \qquad (19)$$

Using Eq. 10 and Eq. 13 this can be rearranged to find an equation for the inlet pressure

$$0.15\left(\frac{\pi W}{4H}\right)^{\frac{5}{3}} ((\rho - \rho_{ice})gH - \Delta p)^{\frac{1}{2}} (\Delta p + C(\rho - \rho_{ice})gH)^{\frac{5}{3}} = \Delta p^{\frac{13}{6}} F(L/H), \qquad (20)$$

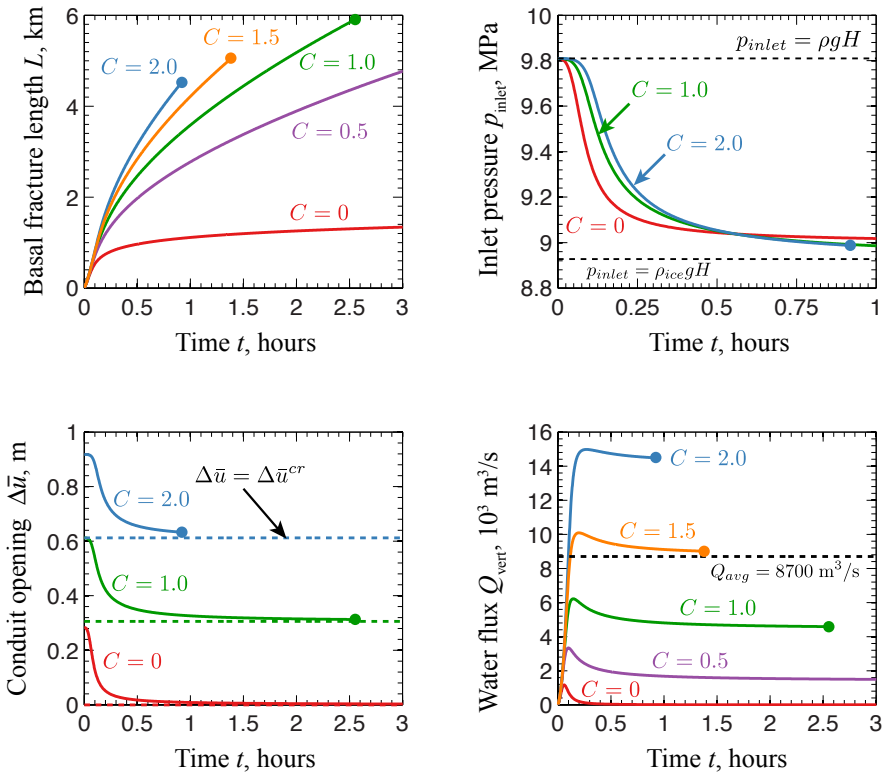

Fig. 5. A plot showing how the basal fracture length, inlet pressure, conduit opening, and water flux into the basal fracture evolve for a range of values of C between 0 and 2.0. Dots at the ends of the curves mark complete drainage of the lake. These results were produced using the parameters given in Tab. 1. We see that the flux into the fracture increases with C, leading to more rapid growth of the basal fracture. The average flux of 8700 m^3/s inferred in [1] is plotted as a dashed line. Our results also show that inlet pressures quickly fall from the initial hydrostatic value to close to σ_o and this is accompanied by elastic closing of the conduit opening.

where we have defined the excess inlet pressure to be $\Delta p = p_{inlet} - \rho_{ice} g H$ and the function

$$F(x) = x^{\frac{7}{6}} \left(1 + 0.125x + 1.218x^2 + 0.129x^3 + 0.189x^4\right). \tag{21}$$

For $C = 0$, Eq. 20 can be solved analytically, allowing p_{inlet} to be written as a function of L. This turns Eq. 6 into a single ordinary differential equation for the length of the basal fracture L that is solved using built-in MATLAB routines. The solution is slightly more complicated when $C \neq 0$ and Eq. 6 and Eq. 20 must be solved simultaneously. It can be shown that Eq. 6 and Eq. 20 form a system of differential-algebraic equations of index 1, leading to two possible solution methods. The first method involves treating Eq. 6 as a single ODE while solving the algebraic equation at each time-step using standard root finding methods, and the second method involves differentiating Eq. 20 with respect to time to yield an ODE for p_{inlet} that is solved alongside Eq. 6. Both methods were tested and found to give consistent results, though all results shown from this point onwards were produced using the root finding method.

Fig. 5 shows the evolution of L and p_{inlet} for the parameters given in Tab. 1 and a range of values of C between zero and two. As shown later, for the largest values of C the lake can completely drain. When total drainage occurs we terminate the solutions and indicate this by a solid circle in Fig. 5. We observe that the basal fracture grows to a length of several kilometers within a few hours, with larger values of C leading to faster fracture growth. This is to be expected since a larger value of C corresponds to a wider vertical conduit, and thus a larger water flux delivered to the basal fracture. Interestingly, we observe that the inlet pressure is relatively insensitive to changes in C, with the inlet pressure typically close to the ice overburden σ_o. However, the sensitive dependence of U_{tip} on the difference between p_{inlet} and σ_o turns this small difference in excess pressure into a pronounced difference in basal fracture length. The small excess pressures shown in Fig. 5 means that elastic opening of the vertical conduit is typically small when compared to the opening due to creep in the period immediately before rapid drainage commences. This is shown in Fig. 5 where we observe that the average conduit opening quickly returns to $\Delta\bar{u} = \Delta\bar{u}^{cr}$ as the inlet pressure falls towards σ_o. We do not show the evolution of conduit opening for $C = 0.5$ and $C = 1.5$ since it is qualitatively similar to the solutions for $C = 0$, 1 and 2, with the average conduit opening falling to $\Delta\bar{u}^{cr}$ over a time scale of approximately half an hour.

Using our solution for L and p_{inlet} we can calculate the water flux from the lake and into the basal fracture using Eq. 13. The evolution of this flux is also shown in Fig. 5. We

observe that at the onset of rapid drainage the flux increases rapidly before reaching a state where the flux remains almost constant. Our results show a strong dependence of the water flux on C, which is to be expected when elastic opening of the vertical conduit is small. Importantly, in the solution for $C = 0$, where creep is neglected and all opening of the conduit is elastic, we see that the conduit quickly closes as the inlet pressure drops preventing the lake from draining. In Fig. 5 we indicate the average water flux of ~ 8700 m^3/s inferred in [1] using a dashed line and find that this is best matched by the solution with $C = 1.5$.

Our calculations for the water flux into the basal fracture can be used to predict how the lake surface height drops once rapid drainage begins. To do this we must first make some assumptions about the geometry of the lake. We assume an axisymmetric lake with a parabolic shape, which allows us to relate the radius of the lake r at a given distance below the lake surface z, where z is taken to be positive in the upwards direction and zero at the initial lake surface. For this parabolic shape,

$$r^2 = \hat{\alpha}(z+D) \quad , \quad \hat{\alpha} = \frac{A_{init}}{\pi D}, \tag{22}$$

where D is the initial lake depth and $\hat{\alpha}$ is a constant determined using observations of the initial lake surface area A_{init}. This allows us to find the area of the lake at any depth z and initial lake volume

$$A(z) = \frac{A_{init}(z+D)}{D} \quad , \quad V_{init} = \frac{DA_{init}}{2}. \tag{23}$$

Thus using the measurements of $A_{init} = 5.6$ km^2 and $V_{init} = 44 \times 10^6$ m^3 from [1] we estimate the initial lake depth to be ~ 15.7 m.

Having approximated the lake geometry and estimated the initial depth we now model the lake drainage using our solution for Q_{vert} and rewrite this in terms of the lake surface height using our solution for $A(z)$ to find

$$\frac{\mathrm{d}V}{\mathrm{d}t} = -Q_{vert}(t) \quad , \quad \frac{\mathrm{d}z}{\mathrm{d}t} = -\frac{DQ_{vert}(t)}{A_{init}(z+D)}. \tag{24}$$

where V is the current volume of water in the lake. To conclude we try to match our model with the observations of a falling lake surface from [1]. Fig. 6 shows how the lake depth drops for the parameters given in Tab. 1 and $C = 2$. To find this optimal value of C we tested a range of values with a spacing of 0.1 We find reasonable agreement with the observational data for the period of most rapid drainage but are unable to match the gradual onset of drainage shown in the data.

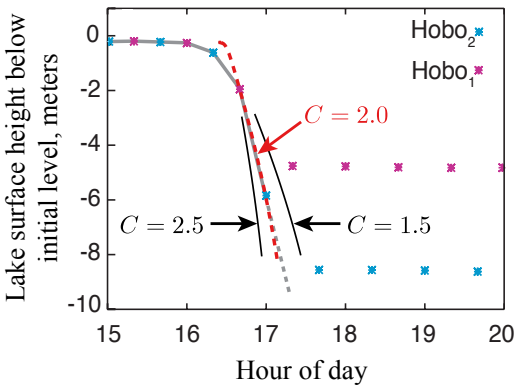

Fig. 6. Data from the 2006 lake drainage event reproduced from Das et al. [1] with an additional curve showing our model prediction for the parameters given in Tab. 1 and $C = 2.0$, meaning that the creep opening is twice what would be the initial elastic opening of the crack-crevasse system if subjected to hydrostatic water pressure.

6 Conclusions

We have reviewed understanding of the coupled fluid and solid mechanics underlying an important class of natural hydraulic fractures, involving rapid lake drainages through and under ice sheets and glaciers by turbulently flowing meltwater.

Our particular focus was on the 2006 rapid drainage event at a well-instrumented supraglacial lake, of $\sim 44 \times 10^6$ m^3 volume, on the Greenland Ice Sheet. Once rapid drainage began, the lake drained into the ice within 1.0 to 1.5 hours.

We showed that our modeling of the drainage time has good correspondence with observational constraints on the rapidity of drainage. Although it is reasonable to assume that the ice responds elastically on such a short time scale, we noted that there was ~ 16 hours of slow drainage (shown by ~ 15 mm/hr fall in lake level), before the breakout to rapid drainage.

Therefore, using standard temperature dependent power-law creep modeling of ice, we quantified possible slow creep opening over that 16 hr period, due to hydrostatic pressurization of a vertical crack-like crevasse system, 2.7 km long as exposed at the surface, which connects the lake bottom to the glacial bed, 1 km below. The crevasse is presumed to be the main conduit for the water.

A creep parameter C was introduced, giving the ratio of the creep opening to what would be the elastic opening of that same vertical crack-crevasse if its surfaces were loaded by hydrostatic fluid pressure. Values of C in the range 1.5 to 2.0 were shown to give an excellent fit to the observations; the former best predicts the average flux of water out of the lake (Fig. 5, lower right), whereas the latter best fits the maximum observed rate of lake level descent (Fig. 6).

Using data on the temperature dependence of creep, we concluded that ice in the vicinity of the lake would have to respond as if it had a temperature in the range -7.0 to -5.0°C to produce such values of C.

GPS measurements were also reported in Figure 2C of [1] and it is not yet clear that our present style of modeling,

Parameter	H	W	ρ	ρ_{ice}	g	k	E'	n	t	A_{cr}(-7°C)	A_{cr}(-5°C)
Value	1	3	1000	910	9.81	0.01	6.8	3	16	6.32×10^{-25}	9.31×10^{-25}
Unit	km	km	kg/m^3	kg/m^3	m/s^2	m	GPa	-	hrs	Pa^{-3}s^{-1}	Pa^{-3}s^{-1}

Table 1. A table summarizing the parameter values used in this manuscript. All parameters choices follow those made in [2] except for the creep parameters which follow [7].

even if improved in sophistication, can fully explain them. They show that the ice sheet was moving primarily to the west with a slight northern trend (at 6% of the westward motion) prior to the rapid drainage event. The event itself caused a rapid 0.8 m displacement of the GPS site to the north, which was followed by its gradual return south over the next two days, after which the primarily westward pre-event motion was recovered.

Based on that pre-event motion, we must assume that the shear traction on the base of the ice sheet was primarily eastward-directed prior to the hydraulic fracture and lake drainage. Further, if the vertical crack/crevasse system (Fig. 1) became highly pressurized over a multi-hour period before the basal hydraulic fracturing, the deformation caused by that pressurization was resisted not just by the stress-dependent creep flow within the ice sheet (which we have modeled here), but also by the development of a component of traction at the base of the ice sheet. That would be a traction component in a direction approximately orthogonal to the pre-event eastward traction, and its development is expected to attenuate the short term creep motion of the ice sheet in a manner consistent with the minimal observed northward displacements at the GPS site prior to the hydraulic fracture. At present, we have no good procedure to describe that process and its effect on the creep opening, which we have modeled here as if there was no basal shear resistance.

However, an assumption of no (or negligible) basal shear resistance is reasonable over the part of the base that is being hydraulically fractured, and hence for assessing the elastic part of the response to crack/crevasse opening. It is clear that a fuller analysis of the basal creep mechanics and shear resistance, in a manner which also rationalizes the GPS observations, is a significant goal for future clarification.

Acknowledgements

This research was supported by the Harvard University School of Engineering and Applied Sciences Blue Hills Hydrology Endowment (MCF), the National Science Foundation, Office of Polar Programs, awards ANT-0739444 (June 2008 to May 2012) and 1341499 (Mar. 2014 to Feb. 2017) to Harvard University.

Nomenclature

A_{init} Initial lake surface area
$A_{cr}(T)$ Power law Creep parameter
$A(z)$ Area of lake cross-section at any depth z
$\hat{\alpha}$ Constant determined using observations
C Ratio of creep to elastic opening of hydrostatically pressurized vertical crevasse
D Initial lake depth at deepest point
$E' = E/(1-\nu^2)$ Effective modulus in plane strain
E Young's modulus
f Darcy-Weisbach friction factor
g Gravitational acceleration
γ Mises equivalent engineering shear strain
H_{Lake} Lake water level
H Uniform ice sheet thickness ($\sim$ 1 km)
$h(x,t)$ Opening gap of basal fracture
$h_{avg}(t)$ Average opening gap of basal fracture
k Nikuradse wall roughness amplitude
K_{Ic} Mode I Fracture toughness of ice
$K_{\alpha\beta}(x,z)$ Erdogan elasticity kernels
$\kappa(n)$ Numerical correction factor depending on n
$L(t)$ Half-length of basal fracture
n Power law creep exponent
ν Poisson Ratio
$p(x,t)$ Basal fluid pressure distribution
$p_{inlet}(t)$ Fluid pressure at basal entry $x = 0$
Δp Excess inlet pressure $p_{inlet} - \sigma_o$
Q Maximum volumetric discharge
Q_{basal} Volumetric discharge rate into basal fracture
Q_{vert} Volumetric discharge rate through vertical crevasse
Re Reynolds Number
R Radius of the basal fracture when assumed circular
r Radius of the lake at a given depth
ρ Mass density of water
ρ_{ice} Mass density of ice
$s_{\alpha\beta}$ Deviatoric stress components
$\sigma_{\alpha\beta}(x,z,t)$ Stress components
σ_o Ice overburden pressure $\rho_{ice} g H$
t Time
T Temperature
τ_{wall} Wall shear stress
τ Mises equivalent shear stress
U Thickness averaged fluid velocity in basal fracture
U_{vert} Thickness averaged fluid velocity in crevasse
U_{tip} Fracture propagation velocity ($= dL/dt$)
$\Delta\bar{u}^{cr}$ Average creep crevasse opening
$\Delta\bar{u}^{el}$ Average elastic crevasse opening
$\Delta\bar{u}(t)$ Average opening gap of vertical crevasse
$\Delta u_\alpha(x,z,t)$ Displacement discontinuities
$V(t)$ Volume in the lake
V_{init} Initial volume of the lake
W Horizontal length of vertical crack-crevasse
x x-axis
y y-axis

z z-axis
Z_{rel} GPS-recorded ice uplift

References

[1] Das, S. B., Joughin, I., Behn, M. D., Howat, I. M., King, M. A., Lizarralde, D., and Bhatia, M. P., 2008. "Fracture propagation to the base of the greenland ice sheet during supraglacial lake drainage". *Science,* **320**, pp. 778–781.

[2] Tsai, V. C., and Rice, J. R., 2010. "A model for turbulent hydraulic fracture and application to crack propagation at glacier beds". *J. Geophys. Res.,* **115**(F03007).

[3] Tsai, V. C., and Rice, J. R., 2012. "Modeling turbulent hydraulic fracture near a free surface". *J. Appl. Mech.,* **79**(3), May.

[4] Adhikari, S., and Tsai, V. C., 2014. "A new model for subglacial flooding during the rapid drainage of supraglacial lakes". Abstract Number C33A-0355, AGU Fall Meeting.

[5] Weertman, J., 1973. "Can a water-filled crevasse reach the bottom surface of a glacier?". *International Association of Hydrologic Sciences,* **IAHS 095 0139**, pp. 139–145.

[6] Tinkler, K., and Marsh, J., 2006. "Niagara river". *The Canadian Encyclopedia*, February.

[7] Cuffey, K., and Patterson, W., 2010. *The Physics of Glaciers*, 4th edition ed. Butterworth- Heinemann, imprint of Elsevier, Burlington, MA.

[8] Needleman, A., and Rice, J. R., 1980. "Plastic creep flow effects in the diffusive cavitation of grain boundaries". *Acta Metallurgica,* **28**(10), pp. 1315–1332.

[9] Bower, A. F., Fleck, N. A., Needleman, A., and Ogbanna, N., 1993. "Indentation of a power law creeping solid". *Proc. Roy. Soc. London Ser. A,* **441**(911), pp. 97–124.

[10] Erdogan, F., Gupta, G. D., and Cook, T. S., 1973. "Numerical solution of singular integral equations". *Leyden, Noordhoff Int. Pub.,* **Recent developments in fracture mechanics, G. C. Sih**, pp. 368–425.

[11] Viesca, R. C., and Rice, J. R., 2011. "Elastic reciprocity and symmetry constraints on the stress field due to a surface-parallel distribution of dislocations". *Journal of the Mechanics and Physics of Solids,* **59**(4), pp. 753–757.

[12] Garagash, D. I., and Detournay, E., 2005. "Plane-strain propagation of a fluid-driven fracture: Small toughness solution". *J. Appl. Mech.,* **72**, pp. 916–928.

[13] Gioia, G., and Chakraborty, P., 2006. "Turbulent friction in rough pipes and the energy spectrum of the phenomenological theory". *Phys. Rev. Lett.,* **96**, pp. 1–4.

[14] Rubin, H., 2001. *Environmental fluid mechanics*. CRC Press.

[15] Nye, J. F., 1953. "The flow law of ice from measurements in glacier tunnels, laboratory experiments and the jungfraufirn borehole experiment". *Proceedings of the Royal Society of London. Series A. Mathematical and Physical Sciences,* **219**(1139), pp. 477–489.

[16] Hutchinson, J., 1968. "Singular behaviour at the end of a tensile crack in a hardening material". *Journal of the Mechanics and Physics of Solids,* **16**(1), pp. 13–31.

[17] Rice, J. R., and Rosengren, G., 1968. "Plane strain deformation near a crack tip in a power-law hardening material". *Journal of the Mechanics and Physics of Solids,* **16**(1), pp. 1–12.

[18] Adhikari, S., and Tsai, V. C., 2015. "A model for subglacial flooding through a preexisting hydrological network during the rapid drainage of supraglacial lakes". *"J. Geophys. Res.",* **120**, doi: 10.1002/2014JF003339.